

RECEIVED BY OSTI

AUG 09 1985

92689

UCRL-
PREPRINT

CONF-8505100--18

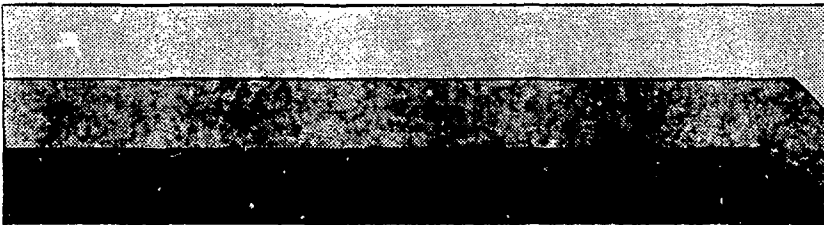
ACCELERATION OF COMPACT TORUS PLASMA RINGS
IN A COAXIAL RAIL-GUNC. W. Hartman
J. H. Hammer
J. Eddleman

UCRL--92689

DE85 016069

This Paper Was Prepared For Submittal to
7th Symposium on Compact
Toroid Research, Santa Fe, NM
May 21 - 23, 1985

May 16, 1985



This is a preprint of a paper intended for publication in a journal or proceedings. Since changes may be made before publication, this preprint is made available with the understanding that it will not be cited or reproduced without the permission of the author.

DISCLAIMER

This report was prepared as an account of work sponsored by an agency of the United States Government. Neither the United States Government nor any agency thereof, nor any of their employees, makes any warranty, express or implied, or assumes any legal liability or responsibility for the accuracy, completeness, or usefulness of any information, apparatus, product, or process disclosed, or represents that its use would not infringe privately owned rights. Reference herein to any specific commercial product, process, or service by trade name, trademark, manufacturer, or otherwise does not necessarily constitute or imply its endorsement, recommendation, or favoring by the United States Government or any agency thereof. The views and opinions of authors expressed herein do not necessarily state or reflect those of the United States Government or any agency thereof.

MASTER

DISTRIBUTION OF THIS DOCUMENT IS UNLIMITED

S

ACCELERATION OF COMPACT TORUS PLASMA RINGS IN A COAXIAL RAIL-GUN*

C. W. Hartman, J. H. Hammer, J. Eddleman[†]
Lawrence Livermore National Laboratory, University of California
Livermore, CA 94550

I. Introduction

We discuss here theoretical studies of magnetic acceleration of Compact Torus⁽¹⁾ plasma rings in a coaxial, rail-gun accelerator as shown in Fig. 1. The rings are formed using a magnetized coaxial plasma gun⁽²⁾ and are accelerated by injection of B_0 flux from an accelerator bank. After acceleration, the rings enter a focusing cone where the ring is decelerated and reduced in radius. As the ring radius decreases, the ring magnetic energy increases until it equals the entering kinetic energy and the ring stagnates.

Scaling laws and numerical calculations of acceleration using a 0-D numerical code are presented. 2-D, MHD simulations are shown which demonstrate ring formation, acceleration, and focusing. Finally, 3-D calculations are discussed which determine the ideal MHD stability of the accelerated ring.

II. Acceleration in a Straight Coax

We consider first, acceleration between straight coaxial electrodes with a lumped circuit \mathcal{L}_x , C driving circuit. The simplified equations describing acceleration are,

$$M \frac{d^2 \rho}{dt^2} = \frac{\mathcal{L}_a' I^2}{2} \quad (1)$$

$$\text{and } \frac{d}{dt} ((\mathcal{L}_x + \mathcal{L}_a' \rho) I) = V_0 - \int \frac{I}{C} dt \quad (2)$$

where $M = \text{constant}$, V_0 is the initial capacitor voltage, $\mathcal{L}_a' = d/d\rho \mathcal{L}_a = 2 \ln r_0/r_i$ and ρ is the position of the ring. A more complete description of the ring motion is used in The Ring Acceleration Code (RAC), which includes drag due to field penetration in the electrodes, and displacement of the plasma CM from the ring field because of plasma motion within the ring during acceleration.

For the straight coax considered here, the magnetic energy of the ring, U_m , does not enter in Eqns. (1) and (2). The maximum normalized acceleration of the ring, $\kappa = M \dot{\rho} / (U_m / L)$, ($L = \text{ring length}$), however, is limited to $\kappa_{\text{max}} \approx 0.2-0.3$ to avoid R-T instability and, consequently, κ_{max} determines the kinetic to magnetic energy ratio $\mathcal{R} = U_k / U_m$ after acceleration if U_m is nearly constant. The decay of U_m due to plasma resistance is calculated in the RAC code by determining the time dependent plasma resistivity accounting for ohmic and compression heating and heating due to changes in acceleration, and for multiple ionization of ions, and losses by line and continuum radiation, thermal conduction.

* Work performed under the auspices of the U.S. Department of Energy by the Lawrence Livermore National Laboratory under contract number W-7405-ENG-48.

[†] Consultant, S. Levy, Inc.

Equations (1) and (2) can be written,

$$r''' = s^2 \quad (1a)$$

$$((1+r)s)''' = -s \quad (1b)$$

where $\tau = t/\lambda_x C$, $r = \rho \lambda_a'/\lambda_x$

$$s = I \left(\lambda_a'^2 C / (2M) \right)^{1/2} \quad \text{and} \quad r' = \frac{dr}{d\tau} .$$

The solutions of (1a) and (2a) with boundary conditions $r = r' = s = 0$ and $S' = S''$, at $\tau = 0$, can be obtained using the RAC code and describe ideal coaxial acceleration. For a fixed accelerator length L_a , the accelerated ring properties are determined by the solution $r(\tau, S_0)$, at $\tau = \tau_a$ (r_a, S_0), where $r_a = \lambda_a/\lambda_x$, $\lambda_a = \lambda_a L_a$. If U_m is constant the quantities of interest for acceleration U_K/U_0 ($U_0 = C V_0/2$) and $U_K L/(U_m k_m L_a)$ can be determined as a function of two parameters λ_x/λ_a and M/M_0 where $M_0 = \lambda_a'^2 C U_0 / \lambda_x$. Fig. 2 plots the quantities versus λ_x/λ_a for $M/M_0 = 0.1, 1.0, 10.0$. Fig. 2 shows that, roughly, a best match of both efficiency $\eta = U_K/U_0$, and kinetic to magnetic energy ratio $\mathcal{R} = U_K L/(U_m k_m L_a)$ is obtained when $M/M_0 \approx 1$ and $\lambda_x/\lambda_a \approx 1$. Larger \mathcal{R} can be achieved, however, at reduced η if $M/M_0 \approx 0.1$. The scaling for straight coax acceleration for $\lambda_x/\lambda_a = 1$ and $M/M_0 = 1$, is given in Table 1.

Table 1 ($L_a = 10^3$ cm, $\lambda_a' = 2$ nh/cm, $M = 10^{-4}$ gm)

U_0 (MJ)	$C(\mu\text{fd})$	V_0 (MV)	$\lambda_x C(\mu\text{sec})$	U_K (MJ)
0.2	25.0	0.13	7.1	0.09
2.0	2.5	1.3	2.3	0.9
20.0	0.25	12.6	0.7	9.0

Table 1 illustrates that scaling to higher energies holding M and L_a fixed requires high voltage drivers quite similar to the Marx-charge banks of high power water-line sources.

Fig. 2 shows that for $\lambda_x/\lambda_a = M/M_0 = 1$, $U_K L/(U_m k_m L_a) \approx 0.6$. If $k_m = 0.25$ the ratio \mathcal{R} is $\mathcal{R} = U_K/U_m = 0.15 L_a/L$. For the example given in Table 1, if $L=10$ cm, $\mathcal{R} = 15$. If the resistive decay of U_m is negligible (hot rings), the focused ring will stagnate at a radius $R_f < R_0/\mathcal{R}$ since $U_m \propto 1/R$. To achieve smaller R_f it is important to increase \mathcal{R} . Large \mathcal{R} can be achieved by causing U_m to decay by forming the ring with high Z plasma ions to increase the radiation losses and maintain low electron temperature. Since $U_m \propto Z_{\text{eff}} / (T_e^{3/2} R^2)$ the ring can be accelerated at large $R = R_0$ and then focused to a smaller R to induce rapid, resistive decay of U_m . Fig. 3 shows RAC calculations of induced decay to achieve $\mathcal{R} = 1.3 \times 10^3$ at $U_0 = 0.2$ MJ. The same process is calculated at higher energies also.

III. 2-D, MHD Simulations of Ring Formation and Acceleration

Fig. 4 shows magnetic surfaces during ring formation for a magnetized plasma gun having roughly the configuration shown in Fig. 1. The surfaces are

calculated using the HAM⁽³⁾, 2-D, MHD code. The ring formation and rapid reconnection of the poloidal field are in approximate agreement with a sharp boundary layer, zero inertia analytic model of formation⁽⁴⁾.

Fig. 5 shows magnetic surfaces during ring acceleration calculated with HAM. The results are in agreement with the ring trajectory described by Eqns. (1) and (2) and illustrate "shaping" of the ring by the $1/R$ variation of the accelerating B_θ field and by the compression of the ring's magnetic field by the accelerated plasma.

Fig. 6 shows magnetic surfaces calculated for a ring undergoing focusing. The results show the predicted, self-similar focusing at low $\beta = P/(B^2/8\pi)$.

IV. 3-D Calculations of Ring Stability During Acceleration

Two numerical codes are used to determine the ideal, MHD equilibrium and stability of an accelerated ring. A linearized, initial value code determines the equilibrium under uniform acceleration and the stability to low azimuthal mode number modes driven by current, pressure, and acceleration. The stability against high mode number, Rayleigh-Taylor like ballooning modes excited by acceleration, is determined by a numerical solution of the eigen-mode equations obtained from an energy principle generalized to include uniform acceleration.

The results suggest a general instability to $M=1$, tilting unless stabilized by line tying by a small amount (10%) of the poloidal flux penetrating the electrodes. 3-D, MHD calculations, however, suggest that the center conductor will limit the tilt to small amplitude.

The stability against pressure and acceleration driven R-T modes is currently under investigation. Preliminary results, which are dependent on the flux distribution ϕ toroidal (ψ_{poloidal}), suggest that reasonable flux distributions are stable for κ 's in the range $\kappa_{\text{max}} = 0.2-0.3$. The 0-D calculations given earlier have been adjusted to have κ_{max} in the stable range.

V. Summary

We have calculated the formation, acceleration, and focusing of Compact Torus plasma rings in a straight coaxial configuration. The models used predict efficient (50%) acceleration within stability limits imposed by the R-T instability. Acceleration to kinetic to magnetic energy ratios $\mathcal{Q} = 10-15$ are predicted for high temperature rings and $\mathcal{Q} = 10^3$ for low temperature rings with magnetic energy decay. The acceleration process is shown to scale in energy from a "proof-of-principle" experiment at 0.2 MJ, to a high energy, 20 MJ, accelerator.

References

1. M. N. Rosenbluth and M. N. Bussac, Nucl. Fusion 19 (1979) 489.
2. H. Alfven, L. Lindberg, and P. Mitlid, J. Nucl. Energy 1 (1960) 116.
3. S. Maxon and J. Eddleman, Phys. Fluids 21 (1978) 1856.
4. J. H. Hammer, Appendix E, LLL-PROP-191, April 15, 1984.

REPRODUCED FROM
BEST AVAILABLE COPY

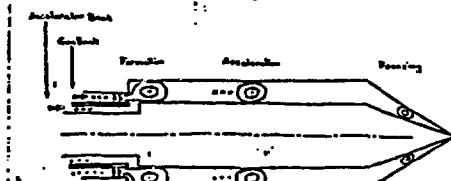


Fig. 1. Coaxial Plasma Ring Accelerator

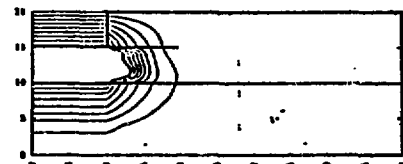
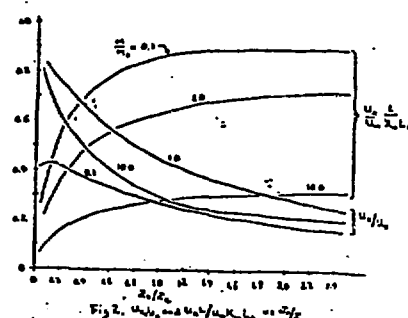


Fig. 4a. Ring Formation, $t = 0.76 \mu s$

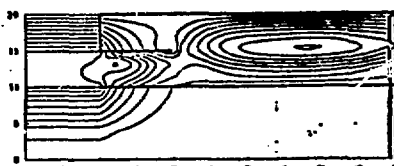


Fig. 4b. Ring Formation, $t = 3.1 \mu s$

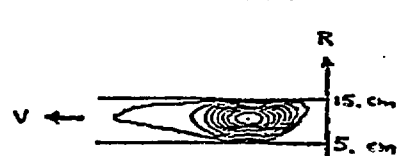
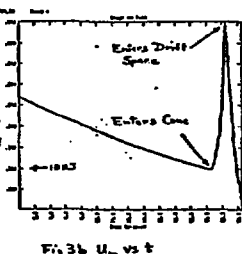
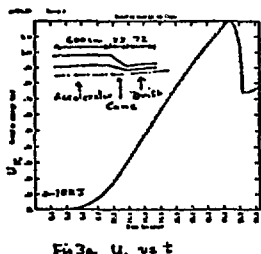


Fig. 5. Accelerated Ring

